Low energy spin dynamics in the spin ice $Ho_2Sn_2O_7$

Low energy spin dynamics in the spin ice Ho$_2$Sn$_2$O$_7$

G Ehlers[1], A Huq[1], S O Diallo[1], C Adriano[2], K C Rule[3], A L Cornelius[4], P Fouquet[5], P G Pagliuso[2] and J S Gardner[6,7]

[1] Neutron Sciences Directorate, Oak Ridge National Laboratory, Oak Ridge, TN 37831-6475, USA
[2] Instituto de Física Gleb Wataghin, Universidade Estadual de Campinas, UNICAMP, 13083-970, Campinas, São Paulo, Brazil
[3] Helmholtz Zentrum Berlin, 14109 Berlin, Germany
[4] Department of Physics, University of Nevada, Las Vegas, NV 89154-4002, USA
[5] Institute Laue–Langevin, 6 rue Jules Horowitz, BP 156, 38042 Grenoble Cedex 9, France
[6] Department of Physics, Indiana University, Bloomington, IN 47408, USA
[7] NCNR, National Institute of Standards and Technology, Gaithersburg, MD 20899-6102, USA

E-mail: ehlersg@ornl.gov

Abstract

The magnetic properties of Ho$_2$Sn$_2$O$_7$ have been investigated and compared to other spin ice compounds. Although the lattice has expanded by 3% relative to the better studied Ho$_2$Ti$_2$O$_7$ spin ice, no significant changes were observed in the high temperature properties, $T \gtrsim 20$ K. As the temperature is lowered and correlations develop, Ho$_2$Sn$_2$O$_7$ enters its quantum phase at a slightly higher temperature than Ho$_2$Ti$_2$O$_7$ and is more antiferromagnetic in character. Below 80 K a weak inelastic mode associated with the holmium nuclear spin system has been measured. The hyperfine field at the holmium nucleus was found to be $\approx$700 T.

(Some figures may appear in colour only in the online journal)

1. Introduction

In a solid state system with localized magnetic moments, unusual low temperature physics can be generated through the well known mechanism of *geometrical frustration*. This frustration is the consequence of the geometric arrangement of the magnetic moments on an underlying crystal lattice that prevents the system from minimizing the energy of all near neighbor bonds simultaneously [1]. The cubic pyrochlore oxides with general chemical composition A$_2$B$_2$O$_7$, where A is a rare-earth ion and B is a transition metal ion, adopt a crystal structure in which both species of ion occupy intertwined networks of corner sharing tetrahedra, which combine to generate one of the prototype lattices known to cause frustration effects [2].

The systems with A = Ho, Dy and B = Ti, Sn adopt a spin ice ground state, which may form when net ferromagnetic near neighbor interactions combine with a local Ising anisotropy on the pyrochlore lattice [3–9]. The defining characteristics of the spin ices are the large residual entropy and non-collinear frozen disordered magnetic moments in the ice phase below the freezing at $T \sim 1$ K, and an extended phase between the ice phase and the paramagnetic phase where spin dynamics is caused by quantum spin tunneling [10, 11]. Pr$_2$Sn$_2$O$_7$ has also been confirmed as a spin ice, but with much faster (by several orders of magnitude) magnetic spin dynamics than the Ho- and Dy-based systems (at $T \simeq 0.2$ K the spin system is not yet frozen in Pr$_2$Sn$_2$O$_7$) [12]. More recently, Dy$_2$Ge$_2$O$_7$ and Ho$_2$Ge$_2$O$_7$ have been synthesized into the cubic pyrochlore form and have been shown to have spin ice character [13].

A lot of detailed research has been carried out on the series of systems with B = Ti, due to the fact that large single crystals can be grown [14] which are suitable for neutron scattering experiments. Some of the rare-earth titanates have become topical materials for their particular ground states. Besides the spin ices, this includes the spin liquid Tb$_2$Ti$_2$O$_7$ [15, 16], and the partially ordered system

Gd$_2$Ti$_2$O$_7$ [17, 18]. On the other hand, the rare-earth based stannates (B = Sn) have only been investigated in detail by a few groups, as they are only available as powders [19, 20]. In this series one finds a similar variety in the ground states, such as seemingly conventional order in Gd$_2$Sn$_2$O$_7$ [21–23], partial order in Tb$_2$Sn$_2$O$_7$ [24, 25], and cooperative paramagnetism in Er$_2$Sn$_2$O$_7$ [26, 27] and Yb$_2$Sn$_2$O$_7$ [20].

Neutron scattering techniques enable detailed insight into the low temperature properties of a material on the atomic scale, because the wavevector and energy dependences of the scattering provide structural and dynamic information simultaneously. The latter is particularly important in the study of frustrated magnets because these systems are generally characterized by a large degeneracy of the ground state which makes them susceptible to low energy fluctuations [28]. For some systems this has been addressed with high resolution neutron techniques such as backscattering (BS) [29–32] or neutron spin echo (NSE) [33–38]. BS works in the energy domain like most inelastic scattering methods, and therefore is sensitive to inelastic processes with small spectral weight, in an energy range between $\sim 10^0$ and $\sim 10^2$ μeV. On the other hand, NSE measures in the time domain, covering a larger dynamic range, between $\sim 10^{-4}$ and $\sim 10^2$ μeV, but is limited in most cases to quasielastic scattering. With NSE one can measure slow spin relaxation processes very well, including an analysis of the line shape of the spin relaxation function in the time domain. Another strength of NSE lies in the use of polarized neutrons, which enables one to separate magnetic and nuclear scattering.

Turning to Ho$_2$Sn$_2$O$_7$, the spin ice character of this system was recognized a long time ago [20, 39, 40]. The Curie–Weiss constant of this material is positive, $\theta_{CW} = +1.8$ K [40]. The near neighbor exchange is also positive, $J_{nn} = 0.30 \pm 0.15$ K [40], in contrast to the titanates [5]. The dipolar energy is $D_{nn} = +2.4$ K [5], placing Ho$_2$Sn$_2$O$_7$ on the spin ice side of the phase diagram for Ising pyrochlore magnets with nearest-neighbor exchange and long-range dipolar interactions [4]. As mentioned earlier, only polycrystalline material is available, which limits the information one can obtain with bulk measurements or with neutron scattering. However, with the recent interest in emergent magnetic monopoles [41, 42] and magnetricity [43], it is important to fully characterize the few materials that are known to form the spin ice ground state. In this paper we present new specific heat and magnetization measurements and a neutron scattering investigation of the spin dynamics in Ho$_2$Sn$_2$O$_7$.

2. Experimental methods

Polycrystalline samples of Ho$_2$Sn$_2$O$_7$ were prepared at the National Institute of Standards and Technology by firing, in air at 1300 °C, stoichiometric amounts of Ho$_2$O$_3$ and SnO$_2$ for several days with intermittent grindings. Room temperature x-ray powder diffraction confirmed a complete reaction and the dearth of impurity phases.

To characterize the magnetic properties, several measurements were performed between 0.3 and 300 K. Uniform susceptibility, ac susceptibility and full magnetic hysteresis loops were measured in a fully calibrated, commercially available measurement system. The heat capacity was measured using a thermal relaxation method between 0.34 and 20 K, and the magnetic contribution was determined after subtracting lattice and nuclear contributions from the measured specific heat.

To further characterize the sample, neutron diffraction was measured at room temperature at the new POWGEN instrument at the spallation neutron source (SNS) at Oak Ridge [44]. The instrument was in commissioning at the time, and three banks of detectors (at $2\theta = 45°$, 85°, 115°) were available to take data. The d-spacings covered by the setup ranged from $d \sim 0.4$ to ~ 4 Å, and the first Bragg peak in range was the (220). The raw detector counts were corrected for efficiency with data taken on a vanadium standard. Rietveld refinements were carried out for all three obtained histograms simultaneously using the FULLPROF package [45].

Neutron spin echo (NSE) was measured at the IN11 instrument in the wide-angle multidetector configuration at the Institute Laue-Langevin (ILL) at Grenoble [35, 46]. A wavelength of $\lambda = 5.5$ Å (15% bandwidth) was used for this experiment. With two positions of the multidetector centered at $2\theta = 20°$ and $50°$, a momentum transfer range from $Q \sim 0.1$ to $Q \sim 1.2$ Å^{-1} was covered. The correlation time range accessible with the experimental setup extended from 4×10^{-12} to 2×10^{-9} s. Data were corrected for instrumental resolution using a magnetic sample that was previously shown to have no spin dynamics in the measurement window [47].

A neutron backscattering experiment was performed at the BASIS instrument at the SNS at Oak Ridge [44, 48]. A polychromatic incident neutron beam was scattered at the sample and then backscattered from an array of Si(111) analyzer crystals into the detector bank, selecting a final neutron energy of 2082 μeV. Operating at $f = 60$ Hz the instrument provided a simultaneous coverage of energy transfer within ± 150 μeV with a resolution of ~ 3.3 μeV at the elastic line. The sample was placed in an orange cryostat, and some additional data were taken at BASIS with a 5 T cryomagnet.

3. Experimental results

Refined neutron powder diffraction patterns are shown in figure 1. The total number of refined reflections was 1943. From the refinement the lattice constant, the 48f x-position, the oxygen site occupation, and the mean-squared displacement parameter for each site were obtained. The final results of the refinement are listed in table 1. The values obtained for the lattice constant and the x parameter are slightly different from previously published data [49] but agree closely with [40]. The oxygen stoichiometry is very close to the ideal value. Overall, the powder diffraction data attest to the good sample quality. The achieved R-factors are in the 5–8% range and are dominated by discrepancies in the peak shape.
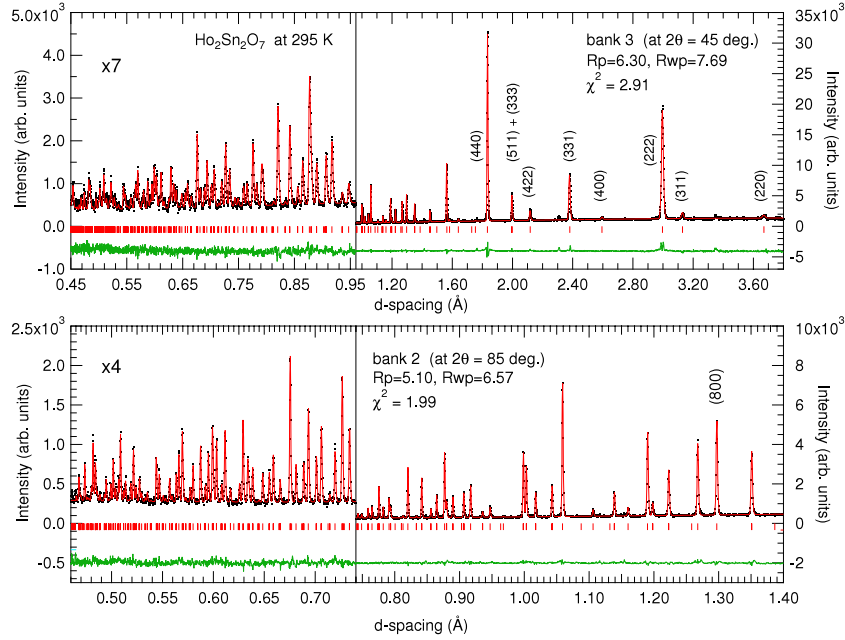
Figure 1. Powder diffraction patterns of $Ho_2Sn_2O_7$ measured at POWGEN. Two banks out of three available banks are shown here.

Table 1. Refinement results from neutron diffraction for the $Ho_2Sn_2O_7$ sample at room temperature.

Position	Atom	Occ.	x, y, z	β_{iso} (Å)
16d	Ho	1	1/2, 1/2, 1/2	0.394(12)
16c	Sn	1	0, 0, 0	0.261(12)
8b	O	0.96(5)	3/8, 3/8, 3/8	0.466(12)
48f	O	0.98(1)	0.336 82(7), 1/8, 1/8	0.380(32)
Symmetry			$Fd\bar{3}m$	
Lattice a			10.375 78(4)	

Bulk measurements are shown in figures 2 and 3. The upper panel of figure 2 compares our measurements of the specific heat of $Ho_2Sn_2O_7$ and $Ho_2Ti_2O_7$ samples after the nuclear and lattice contributions have been subtracted. Comparing the two datasets, the maximum of the specific heat of $Ho_2Sn_2O_7$ is at a slightly lower temperature than in $Ho_2Ti_2O_7$, but they have similar peak heights. This shift in peak position is a result of a more antiferromagnetically coupled system, as discussed in [4]. Integrating $C(T)/T$ of $Ho_2Sn_2O_7$ between $T = 0.4$ and 23 K one arrives at an entropy difference of $\Delta S = 3.89$ J mol^{-1} K$^{-1} \sim 0.68R \ln(2)$, nearly identical to the value obtained for $Dy_2Ti_2O_7$ [3]. The real and imaginary parts of the ac susceptibility are shown in the lower panel of figure 2. In our measurements, the imaginary part peaks at 1.2 K, which is in good agreement with Matsuhira's data [39]. Again, spin freezing sets in at a few tenths of a degree lower temperature than in $Ho_2Ti_2O_7$.

To investigate the high temperature regime of $Ho_2Sn_2O_7$, $T \gtrsim 10$ K, one has to apply a uniform dc field to the polycrystalline sample, otherwise the temperature dependence above 5 K appears Curie–Weiss like, see figure 3(a). A similar approach is necessary for $Ho_2Ti_2O_7$ [50]. The 12 K freezing process seen in $Ho_2Sn_2O_7$ has similar characteristics to that of
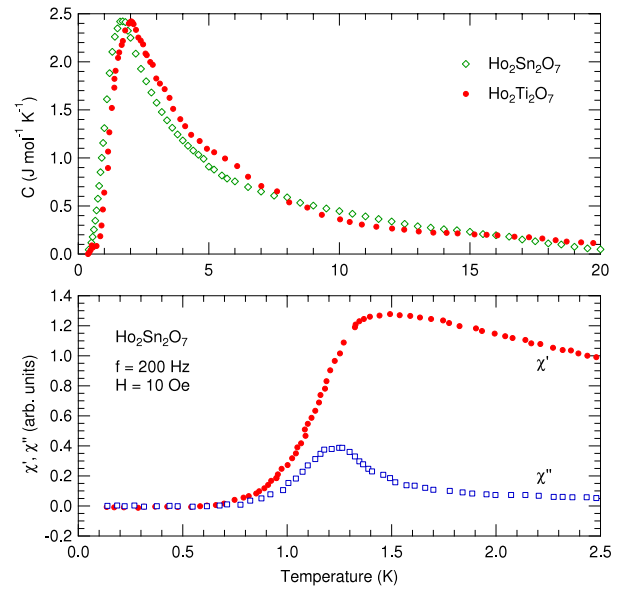
Figure 2. Upper panel: specific heat data for $Ho_2Sn_2O_7$ and $Ho_2Ti_2O_7$. Lower panel: real and imaginary parts of the dynamical susceptibility of $Ho_2Sn_2O_7$ measured at 200 Hz around the macroscopic spin freezing temperature.

$Ho_2Ti_2O_7$ which is interpreted as a freezing of the thermally activated spin flip process via the lowest lying crystal field excitations, as discussed earlier [10, 51]. In measurements of the field dependent magnetization $M(H)$ one can see the effects of spin correlation (deviations from paramagnetic behavior) in $Ho_2Sn_2O_7$ around 10 K, see figure 3(b). In the low temperature isotherms one also sees that within our field range the system almost reaches saturation with the maximum magnetization at $\sim 5 \mu_B$ or half the Ho^{3+} saturated moment
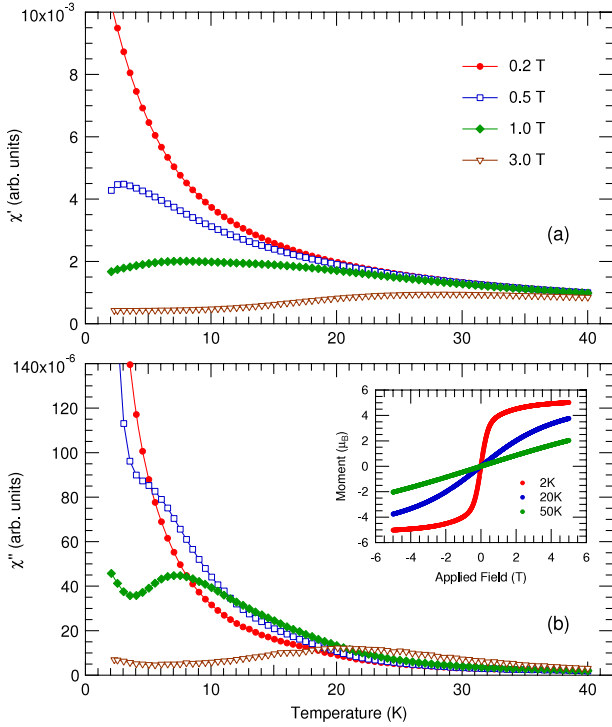
Figure 3. Real and imaginary parts of the ac susceptibility in an applied dc field. The inset shows the field dependent magnetization at three temperatures.
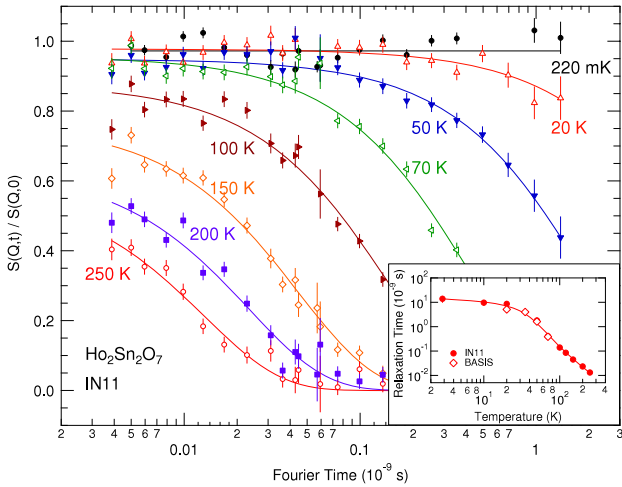

Figure 4. Neutron spin echo measurements. The lines are fits to a single exponential relaxation function. The inset shows the temperature dependence of the fitted relaxation times (reciprocal rates).

Figure 5. Backscattering spectra combined with NSE spectra at the same temperature.

as expected in two level polycrystalline samples with strong axial anisotropy [50, 52].

A different perspective on the low temperature spin dynamics is gained from quasielastic neutron scattering data, as shown in figures 4 and 5. In these figures, the error bars represent $\pm 1\sigma$ from counting statistics. The spin dynamics is characterized by the dominance of a single, temperature-dependent, time scale in the relaxation spectrum, similar to the case of the canonical spin ice $Ho_2Ti_2O_7$ [10, 51].
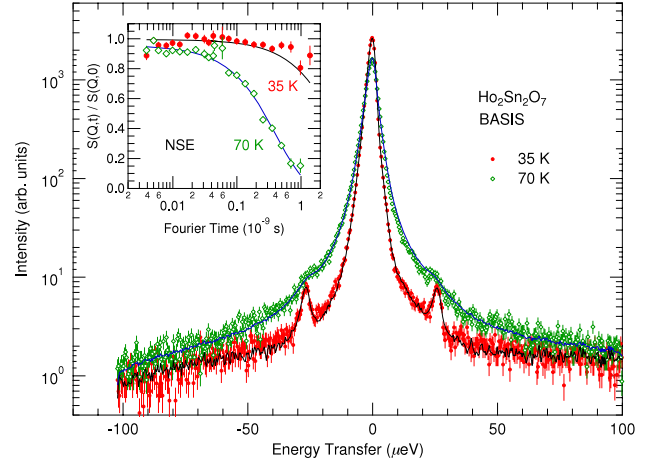
This time scale was found to be independent of Q in the range studied, indicating a single ion relaxation process as expected for a spin ice. Good fits to the data could be obtained with a single exponential relaxation function,

$$I(Q, t)/I(Q, 0) = A \exp(-\Gamma(T)t), \qquad (1)$$

where the prefactor A is proportional to the number of static spins in the experimental system. An analysis of the temperature dependence of the relaxation rates reveals a transition between two different regimes around $T \sim 35$ K. At higher temperature the spin dynamics is thermally activated, as evidenced by an Arrhenius-like temperature dependence of the fitted relaxation rates,

$$\Gamma(T) = 2\Gamma_0 \exp(-E_a/k_B T), \qquad (2)$$

where $\Gamma_0 = (7.8 \pm 0.4) \times 10^{10}$ Hz and $E_a = (277 \pm 4)$ K. These values are similar to those found for $Ho_2Ti_2O_7$ [51], using neutron scattering, and the energy barrier E_a is likely associated with the crystal field splitting between the ground state doublet and the first excited state of the Ho^{3+} ion in the crystal electric field [10]. According to figure 5, [40], this splitting is 22 meV (250 K). The physical picture of the spin relaxation mechanism is that the spin flips between the two states of the ground state doublet (a 180° spin flip) and the energy of the first excited state provides a barrier that has to be overcome. Note that with bulk measurements a very different energy barrier has been obtained [39], but this is in fact not surprising given that ac susceptibility measures the dynamics on a very different time scale which is many orders of magnitude slower. Above $T \sim 35$ K it is also observed that the prefactor A starts to deviate noticeably from 1. This may be explained, at least in part, by the observation that the spin dynamics becomes increasingly faster with increasing temperature, and moves out of the measurement window of the spin echo apparatus. The fit may thus be more and more susceptible to small deviations from the assumed line shape. However, it is also possible that different, much faster relaxation mechanisms emerge at high temperature, when the temperature becomes comparable to the first and higher crystal field states of the Ho^{3+} ion.

On cooling below $T \sim 35$ K, on the other hand, the system enters a plateau and the dynamics, while still detectable, does not appreciably change down to 2 K. This indifference to temperature is characteristic of a quantum tunneling relaxation process and has been seen in $Ho_2Ti_2O_7$ [10]. However, recent analysis of magnetic monopole propagation through the lattice by Jaubert and Holdsworth [53, 54] could also account for this regime.

The combination of NSE and backscattering results validates the results obtained above. Figure 5 shows BASIS data with a simultaneous fit to spin echo data measured at the same temperature. The dynamics associated with the Ho^{3+} electronic magnetic moments manifests itself in the line width of the central line of the backscattering data. The backscattering data further reveal the presence of two small excitation peaks at ±26.3 μeV. These peaks are invisible in the NSE data for two reasons. First of all, the intensity is too low (less than 1% of the quasielastic scattering), and secondly, these peaks are due to nuclear scattering to which the NSE experimental setup is not sensitive [35]. These peaks are discussed in more detail below.

A simultaneous fit to NSE and backscattering data was achieved by writing down the scattering functions as

$$\text{(NSE)} \frac{I(Q, t)}{I(Q, 0)} = A \exp(-\Gamma(T)t),$$
$$\text{(BS)} S(Q, \omega) = I_M \left\{ A \frac{\hbar\Gamma}{(\hbar\Gamma)^2 + (\hbar\omega)^2} + (1 - A)\delta(\omega) \right\} \quad (3)$$
$$+ I_{HF}\{\delta(-\hbar\omega_0) + \delta(+\hbar\omega_0)\} + I_N\delta(\omega),$$

where the prefactor A, $0 \leq A \leq 1$, splits the observed magnetic intensity into a dynamic part (giving rise to quasielastic scattering), and an elastic part $\sim(1 - A)$. The different scattering processes correspond to the observed intensities I_M (magnetic), I_N (nuclear elastic) and I_{HF} (peaks at $\hbar\omega_0 = 26.3$ μeV). As above, τ is the magnetic relaxation time and $\Gamma = \hbar/\tau$. Note that A can be assumed to be the same for both the backscattering and the spin echo experiments, since the neutron energy used and the energy resolution achieved were about the same, and therefore the same part of the magnetic relaxation spectrum was probed. The nuclear scattering processes ($\sim I_{HF}, I_N$) do not appear in the NSE scattering function because the apparatus separates out the magnetic scattering by neutron polarization analysis. Likewise, the $(1 - A)\delta(\omega)$ term corresponds in NSE to an initial drop of the signal below 1, at a correlation time outside the measurement window. The detailed balance factor can be neglected in the above equations because $\hbar\omega \ll k_BT$. The numerical convolution of the scattering function in the energy domain, $S(Q, \omega)$, with the elastic resolution function of the backscattering spectrometer, was fitted to the experimental backscattering data, and the sum of the normalized χ^2 for both datasets minimized.

The discussion now turns to the small inelastic peaks in the backscattering data at ±26.3 μeV. In a reference measurement, performed at BASIS with the sample held in a magnetic field of 5 T at 1.5 K, no change to the intensity or energy of the small peaks was detectable (not shown in a figure). Likewise it was found that the intensity and energy
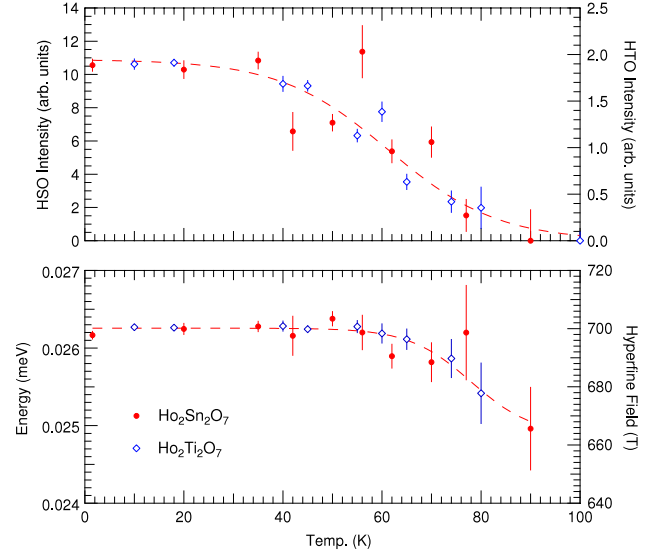

Figure 6. Temperature dependence of the intensity (upper panel) and energy (lower panel) of the 26 μeV peaks. Data for $Ho_2Ti_2O_7$ are included for comparison from [32]. The lines are guides to the eye.

of the peaks are independent of Q, which is analogous to the $Ho_2Ti_2O_7$ case [55]. This leads to the conclusion that the peaks are due to transitions between states with different quantum number m of the nuclear Ho spin in the hyperfine (hf) field (a selection rule $\Delta m = \pm1$ applies) [32]. From the numerical value of the magnetic moment of the Ho nucleus, a magnitude of the hyperfine field of ~700 T can be inferred for $Ho_2Sn_2O_7$, which is comparable to pure Ho metal (770 T).

This interpretation is consistent with the observed temperature evolution of the peak intensity, which is shown in figure 6. Transitions between different states of the Ho nucleus in the hf field can only be observed in a situation where the hf field itself (which has the same fluctuation rate as the electronic magnetic moment) can be considered static. In other words, the Larmor frequency of the Ho nuclear moment in the hf field, which is about $\nu_L \sim 6.36$ GHz (the gyromagnetic ratio of the Ho nucleus is equal to $\gamma/2\pi = 9.06$ MHz T^{-1}), must be much faster than the electronic spin fluctuation rate. The latter is well described by the Arrhenius law, and with the numbers for E_a and Γ_0 derived above one arrives at a critical temperature of $T_L \sim 87$ K at which the Larmor frequency ν_L matches the spin fluctuation rate. Thus, only at $T \ll 87$ K does one expect to see peaks due to hf field transitions with full intensity, and at intermediate temperature the peaks are expected to vanish, which is exactly what one observes. The energy at which the peaks are observed softens a little in the temperature range of the measurement, reflecting a nearly temperature independent magnitude of the hyperfine field [32].

4. Conclusions

We have studied the spin ice $Ho_2Sn_2O_7$ with specific heat, magnetic susceptibility and dynamic neutron scattering experiments, complementing an earlier study [40]. It turns

out that this material is in many aspects nearly identical to the prototypical spin ice, $Ho_2Ti_2O_7$. The magnetic heat capacity has a broad maximum at 1.7 K but otherwise lacks any indication for a phase transition to an ordered state, down to 0.4 K. The entropy difference between the low temperature ice phase, $T \sim 0.4$ K, and the high temperature paramagnetic phase, $T \sim 23$ K, is $\Delta S \sim 0.68R \ln(2)$, and in the paramagnetic regime of $Ho_2Sn_2O_7$, the spin system relaxes on a time scale nearly identical to $Ho_2Ti_2O_7$ ($\tau \sim$ 1 ns at 50 K). Again, like in $Ho_2Ti_2O_7$, between the paramagnetic and the ice phases one observes a phase with slow, quantum-like spin dynamics on the nanosecond time scale. In $Ho_2Sn_2O_7$ this phase might extend to higher temperatures but a more detailed low-T study is required to confirm this.

It was also possible to access the nuclear spin dynamics with modern neutron scattering instrumentation. A weak neutron scattering process, visible at low temperature at an energy $\hbar\omega = \pm 26.3$ μeV, was identified with a $\Delta m = \pm 1$ transition of the Ho nuclear spin in the hyperfine field.

To summarize, the larger lattice of $Ho_2Sn_2O_7$ over $Ho_2Ti_2O_7$, resulting in an $\approx 3\%$ increase in the Ho–Ho bond distance, does not affect the high temperature paramagnetic properties, $T \gtrsim 35$ K. There is some evidence that the quantum-like state is entered at a higher temperature in $Ho_2Sn_2O_7$ but the spin ice ground state is entered at approximately the same temperature (1.7 K). These data have expanded on previous work by Matsuhira *et al* [39, 40] and the high resolution neutron scattering also revealed the nuclear spin system. We have shown that the two Ho-based spin ices are nearly identical and we hope that these studies will motivate chemists to grow single crystals of the title compound so that more detailed investigations of monopole-like quasiparticles can be performed.

Acknowledgments

References

[1] Gardner J S, Gingras M J P and Greedan J E 2010 Magnetic pyrochlore oxides *Rev. Mod. Phys.* **82** 53–107
[2] Subramanian M A, Aravamudan G and Subba Rao G V 1983 Oxide pyrochlores—a review *Prog. Solid State Chem.* **15** 55–143
[3] Ramirez A P, Hayashi A, Cava R J, Siddharthan R and Shastry B S 1999 Zero-point entropy in 'spin ice' *Nature* **399** 333–5
[4] den Hertog B C and Gingras M J P 2000 Dipolar interactions and origin of spin ice in Ising pyrochlore magnets *Phys. Rev. Lett.* **84** 3430–3
[5] Bramwell S T and Gingras M J P 2001 Spin ice state in frustrated magnetic pyrochlore materials *Science* **294** 1495–501
[6] Bramwell S T *et al* 2001 Spin correlations in $Ho_2Ti_2O_7$: a dipolar spin ice system *Phys. Rev. Lett.* **87** 047205
[7] Fennell T, Petrenko O A, Fak B, Bramwell S T, Enjalran M, Yavors'kii T, Gingras M J P, Melko R G and Balakrishnan G 2004 Neutron scattering investigation of the spin ice state in Dy(2)Ti(2)O(7) *Phys. Rev.* B **70** 134408
[8] Morris D J P *et al* 2009 Dirac strings and magnetic monopoles in the spin ice Dy(2)Ti(2)O(7) *Science* **326** 411–4
[9] Fennell T, Deen P P, Wildes A R, Schmalzl K, Prabhakaran D, Boothroyd A T, Aldus R J, McMorrow D F and Bramwell S T 2009 Magnetic Coulomb phase in the spin ice Ho(2)Ti(2)O(7) *Science* **326** 415–7
[10] Ehlers G, Cornelius A L, Orendáč M, Kajňaková M, Fennell T, Bramwell S T and Gardner J S 2003 Dynamical crossover in 'hot' spin ice *J. Phys.: Condens. Matter* **15** L9–15
[11] Snyder J, Ueland B G, Mizel A, Slusky J S, Karunadasa H, Cava R J and Schiffer P 2004 Quantum and thermal spin relaxation in the diluted spin ice $Dy_{2-x}M_xTi_2O_7$ (M = Lu, Y) *Phys. Rev.* B **70** 184431
[12] Zhou H D, Wiebe C R, Janik J A, Balicas L, Yo Y J, Qiu Y, Copley J R D and Gardner J S 2008 Dynamic spin ice: $Pr_2Sn_2O_7$ *Phys. Rev. Lett.* **101** 227204
[13] Zhou H D *et al* 2011 High pressure route to generate magnetic monopole dimers in spin ice *Nature Commun.* **2** 478
[14] Gardner J S, Gaulin B D and Paul D M 1998 Single crystal growth by the floating-zone method of a geometrically frustrated pyrochlore antiferromagnet, $Tb_2Ti_2O_7$ *J. Cryst. Growth* **191** 740–5
[15] Gardner J S *et al* 1999 Cooperative paramagnetism in the geometrically frustrated pyrochlore antiferromagnet $Tb_2Ti_2O_7$ *Phys. Rev. Lett.* **82** 1012–5
[16] Mirebeau I, Goncharenko I N, Cadavez-Pares P, Bramwell S T, Gingras M J P and Gardner J S 2002 Pressure-induced crystallization of a spin liquid *Nature* **420** 54–7
[17] Champion J D M, Fennell T, Wills A S, Bramwell S T, Gardner J S and Green M A 2001 Order in the Heisenberg pyrochlore: the magnetic structure of $Gd_2Ti_2O_7$ *Phys. Rev.* B **64** 140407
[18] Stewart J R, Ehlers G, Wills A S, Bramwell S T and Gardner J S 2004 Phase transitions, partial disorder and multi-k structures in $Gd_2Ti_2O_7$ *J. Phys.: Condens. Matter* **16** L321–6
[19] Bondah-Jagalu V and Bramwell S T 2001 Magnetic susceptibility study of the heavy rare-earth stannate pyrochlores *Can. J. Phys.* **79** 1381–5
[20] Matsuhira K, Hinatsu Y, Tenya K, Amitsuka H and Sakakibara T 2002 Low-temperature magnetic properties of pyrochlore stannates *J. Phys. Soc. Japan* **71** 1576–82
[21] Wills A S, Zhitomirsky M E, Canals B, Sanchez J P, Bonville P, de Réotier P D and Yaouanc A 2006 Magnetic ordering in Gd(2)Sn(2)O(7): the archetypal Heisenberg pyrochlore antiferromagnet *J. Phys.: Condens. Matter* **18** L37–42
[22] Quilliam J A, Ross K A, Del Maestro A G, Gingras M J P, Corruccini L R and Kycia J B 2007 Evidence for gapped spin-wave excitations in the frustrated $Gd_2Sn_2O_7$ pyrochlore antiferromagnet from low-temperature specific heat measurements *Phys. Rev. Lett.* **99** 097201
[23] Stewart J R, Gardner J S, Qiu Y and Ehlers G 2008 Collective dynamics in the heisenberg pyrochlore antiferromagnet $Gd_2Sn_2O_7$ *Phys. Rev.* B **78** 132410
[24] Mirebeau I, Apetrei A, Rodríguez-Carvajal J, Bonville P, Forget A, Colson D, Glazkov V, Sanchez J P, Isnard O and Suard E 2005 Ordered spin ice state and magnetic fluctuations in $Tb_2Sn_2O_7$ *Phys. Rev. Lett.* **94** 246402
[25] Rule K C *et al* 2007 Polarized inelastic neutron scattering of the partially ordered $Tb_2Sn_2O_7$ *Phys. Rev.* B **76** 212405
[26] Lago J, Lancaster T, Blundell S J, Bramwell S T, Pratt F L, Shirai M and Baines C 2005 Magnetic ordering and

dynamics in the XY pyrochlore antiferromagnet: a muon-spin relaxation study of Er(2)Ti(2)O(7) and Er(2)Sn(2)O(7) *J. Phys.: Condens. Matter* **17** 979–88

[27] Sarte P M, Silverstein H J, Van Wyk B T K, Gardner J S, Qiu Y, Zhou H D and Wiebe C R 2011 Absence of long-range magnetic ordering in the pyrochlore compound $Er_2Sn_2O_7$ *J. Phys.: Condens. Matter* **23** 382201

[28] Gardner J S, Ehlers G, Bramwell S T and Gaulin B D 2004 Spin dynamics in geometrically frustrated antiferromagnetic pyrochlores *J. Phys.: Condens. Matter* **16** S643–51

[29] Mondelli C, Mutka H, Frick B and Payen C 1999 Spin freezing in the kagome system $SrCr_8Ga_4O_{19}$—high resolution study of the elastic and low-energy dynamic responses *Physica* B **266** 104–7

[30] Mirebeau I, Mutka H, Bonville P, Apetrei A and Forget A 2008 Investigation of magnetic fluctuations in $Tb_2Sn_2O_7$ ordered spin ice by high-resolution energy-resolved neutron scattering *Phys. Rev.* B **78** 174416

[31] Clancy J P, Ruff J P C, Dunsiger S R, Zhao Y, Dabkowska H A, Gardner J S, Qiu Y, Copley J R D, Jenkins T and Gaulin B D 2009 Revisiting static and dynamic spin-ice correlations in Ho(2)Ti(2)O(7) with neutron scattering *Phys. Rev.* B **79** 014408

[32] Ehlers G, Mamontov E, Zamponi M, Kam K C and Gardner J S 2009 Direct observation of a nuclear spin excitation in $Ho_2Ti_2O_7$ *Phys. Rev. Lett.* **102** 016405

[33] Pouget S and Alba M 1999 NSE investigation of the spin dynamics in the nearly percolating frustrated insulating compound $CdCr_{2(1-x)}In_{2x}S_4$ ($x = 0.10$) *Physica* B **267/268** 304–7

[34] Pappas C, Mezei F, Ehlers G, Manuel P and Campbell I A 2003 Dynamic scaling in spin glasses *Phys. Rev.* B **68** 054431

[35] Ehlers G 2006 Study of slow dynamic processes in magnetic systems by neutron spin-echo spectroscopy *J. Phys.: Condens. Matter* **18** R231–44

[36] Mutka H, Ehlers G, Payen C, Bono D, Stewart J R, Fouquet P, Mendels P, Mevellec J Y, Blanchard N and Collin G 2006 Neutron spin-echo investigation of slow spin dynamics in kagom[e-acute]-bilayer frustrated magnets as evidence for phonon assisted relaxation in $SrCr_{9x}Ga_{12-9x}O_{19}$ *Phys. Rev. Lett.* **97** 047203

[37] Rule K C, Ehlers G, Gardner J S, Qiu Y, Moskvin E, Kiefer K and Gerischer S 2009 Neutron scattering investigations of the partially ordered pyrochlore $Tb_2Sn_2O_7$ *J. Phys.: Condens. Matter* **21** 486005

[38] Gardner J S, Ehlers G, Fouquet P, Farago B and Stewart J R 2011 Slow and static spin correlations in $Dy_{2+x}Ti_{2-x}O_{7-\delta}$ *J. Phys.: Condens. Matter* **23** 164220

[39] Matsuhira K, Hinatsu Y, Tenya K and Sakakibara T 2000 Low temperature magnetic properties of frustrated pyrochlore ferromagnets $Ho_2Sn_2O_7$ and $Ho_2Ti_2O_7$ *J. Phys.: Condens. Matter* **12** L649–56

[40] Kadowaki H, Ishii Y, Matsuhira K and Hinatsu Y 2002 Neutron scattering study of dipolar spin ice $Ho_2Sn_2O_7$: frustrated pyrochlore magnet *Phys. Rev.* B **65** 144421

[41] Ryzhkin I A 2005 Magnetic relaxation in rare-earth oxide pyrochlores *J. Exp. Theor. Phys.* **101** 481–6

[42] Castelnovo C, Moessner R and Sondhi S L 2008 Magnetic monopoles in spin ice *Nature* **451** 42–5

[43] Bramwell S T, Giblin S R, Calder S, Aldus R, Prabhakaran D and Fennell T 2009 Measurement of the charge and current of magnetic monopoles in spin ice *Nature* **461** 956–U211

[44] Mason T E *et al* 2006 The Spallation Neutron Source in Oak Ridge: a powerful tool for materials research *Physica* B **385/386** 955–60

[45] Rodríguez-Carvajal J 1993 Recent advances in magnetic structure determination by neutron powder diffraction *Physica* B **152** 55–69

[46] Farago B 1997 IN11C, medium-resolution multidetector extension of the IN11 NSE spectrometer at the ILL *Physica* B **241** 113–6 (International Conference on Neutron Scattering, Toronto, Canada)

[47] Ehlers G *et al* 2006 Dynamics of diluted ho spin ice $Ho_{2-x}Y_xTi_2O_7$ studied by neutron spin echo spectroscopy and ac susceptibility *Phys. Rev.* B **73** 174429

[48] Mamontov E and Herwig K W 2011 A time-of-flight backscattering spectrometer at the spallation neutron source, basis *Rev. Sci. Instrum.* **82** 085109

[49] Kennedy B J 1997 Structural and bonding trends in tin pyrochlore oxides *J. Solid State Chem.* **130** 58–65

[50] Cornelius A L and Gardner J S 2001 Short-range magnetic interactions in the spin-ice compound $HO_2Ti_2O_7$ *Phys. Rev.* B **64** 060406

[51] Ehlers G, Cornelius A L, Fennell T, Koza M, Bramwell S T and Gardner J S 2004 Evidence for two distinct spin relaxation mechanisms in 'hot' spin ice $Ho_2Ti_2O_7$ *J. Phys.: Condens. Matter* **16** S635–42

[52] Bramwell S T, Field M N, Harris M J and Parkin I P 2000 Bulk magnetization of the heavy rare earth titanate pyrochlores—a series of model frustrated magnets *J. Phys.: Condens. Matter* **12** 483–95

[53] Jaubert L D C and Holdsworth P C W 2009 Signature of magnetic monopole and Dirac string dynamics in spin ice *Nature Phys.* **5** 258–61

[54] Jaubert L D C and Holdsworth P C W 2011 Magnetic monopole dynamics in spin ice *J. Phys.: Condens. Matter* **23** 164222

[55] Ehlers G, Mamontov E, Zamponi M and Gardner J S 2010 Low lying spin excitation in the spin ice, $Ho_2Ti_2O_7$ *J. Phys.: Conf. Ser.* **251** 012003